BULLETIN OF THE POLISH ACADEMY OF SCIENCES
TECHNICAL SCIENCES, Vol. 59, No. 4, 2011
DOI: 10.2478/v10175-011-0066-2

A robust 18-pulse diode rectifier with coupled reactors

P. MYSIAK[1*] and R. STRZELECKI[1,2]

[1] Faculty of Electrical Engineering, Gdynia Maritime University, Department of Ship Automation, 81-87 Morska St., 81-225 Gdynia, Poland
[2] Electrotechnical Institute, Department of Power Converters, 28 Pożaryskiego St., 04-703 Warsaw, Poland

Abstract. The article presents the principle of operation and selected results of simulation and laboratory tests of the 18-pulse rectifier system with coupled reactors and small series active power filter. The presented system makes it possible to reduce, especially in distribution supply networks, undesired higher current harmonics. The 18-pulse nature of operation of the rectifier is reached using a set of coupled three-phase network reactors (CDT and CTR). The simultaneous use of the coupled reactors and the small active power filter provides opportunities for reduction of the supply current distortion, especially in case of voltage harmonic distortion and voltage unbalance.

Key words: series active power filters, multi-pulse rectifiers, coupled reactors, power conditioning.

1. Introduction

The quality of electric energy (EE) reception, most frequently evaluated using the Power Factor γ and the Total Harmonic Distortion coefficient *THD*(I), is of extreme importance in case of supply systems with small short-circuit powers, as compared to the load power [1]. Such power relations between the source and the load are observed, for instance, in autonomous (island) systems. This also may refer to some local distributed supply installations with remarkable proportion of renewable sources, in operation in unfavourable ambient conditions, bad weather for instance [2].

Improving the quality of EE reception in the existing installations is usually obtained by connecting additional filtering and/or compensating devices [3, 4]. On the other hand, in newly designed installations a tendency is to use receivers having the power factor $\gamma \approx 1$, i.e. the phase shift φ and *THD*(I) of the received current close to zero. Among them, due to their application range a special role is attributed to AC-DC converters operating in conditions close to CPC (Clean Power Converter) [5–11]. As frequently as possible, uncontrolled (diode) converters are used which do not impose remarkable reliability problems and reveal low level of emission of high-frequency disturbances.

A non-transformer 18-pulse diode rectifier with coupled reactors, which has characteristics close to CPC and is preferably designed for LV networks is presented in [12, 13]. In nominal supply conditions this rectifier reveals the quality of EE reception close to that represented by other 18-pulse converters with transformers or autotransformers [6, 11]. Its advantage is a much smaller limiting power of the required electromagnetic elements, which obviously results in smaller dimensions and weight of the entire rectifying device. Unfortunately, the rectifier with coupled reactors reveals small resistance to voltage disturbances in the supply network. Distortion or unbalance of this voltage seriously worsens the quality of EE reception.

The discussion of the effect of the distortion and unbalance of the supply voltage on the quality of the EE received by the rectifier with coupled reactors is the first basic goal of the article. The second goal is to present the results of the examination of such an integrated 18-pulse rectifier with a series active filter (S-APF), which reveals improved resistance to supply disturbances.

2. The basic system of 18-pulse rectifier with coupled reactors

Figure 1 presents a basic supply system which makes use of an 18-pulse diode rectifier with coupled three-phase reactors. This and similar AC-DC converters operate at the leading DC load [12–14]. The three-phase supply network is represented by the source voltage e and the line impedance Z_s. Moreover, reactors of inductance L_d are connected in series to the supply source, to reduce the amplitude of higher harmonics of the network currents.

The basic assumption in the adopted concept of the presented system is the construction of three vectors of 3-phase voltages supplying the bridge rectifiers, with the phase shifted by 20°. In this case, the voltage ν_K at the input terminals of the converter takes the 18-step shape at nominal load. The voltages ν_K measured between the terminals K and the neutral point 0 can be interpreted as the result of cyclic switching of V_{DC} voltage (Fig. 1) via the diodes of three bridge rectifiers. The 18-pulse waveform of the voltages ν_K (Fig. 2) is only obtained when the diode conduction angles are equal to π, and when the conduction intervals (18 intervals) are symmetrically distributed along the supply voltage period. In this case the three-phase bridge rectifiers generate a three-level voltage at the AC terminals. The phase voltages at terminals $D2$ are by 20° ahead of the relevant phase voltages at terminals $D1$. In turn, the phase voltages at terminals $D3$ are phase-delayed by 20° with phase voltages at terminals $D1$. As a consequence, the coupled three-phase reactor (CTR) ex-

*e-mail: mysiak@am.gdynia.pl

ecutes 40° phase shift between two output voltage systems. The applied electromagnetic systems – current dividing transformer (CDT) and (CTR) make it possible to obtain the required distribution of the network current on bridge rectifiers. The overall effect of the operation of the coupled reactors is converting the three-phase voltage of the supply source into the nine-phase voltage.

Figure 3 shows a simplified model of the tested system (Figure 1), which allows for qualitative assessment of the impact of its parameters, and the impact of voltage disturbances on the input current distortion. Although it assumes full symmetry of the system, this model can also be applied for assessing the effect of unbalance of supply voltages. This unbalance is a source of additional distortions of voltages v_K.

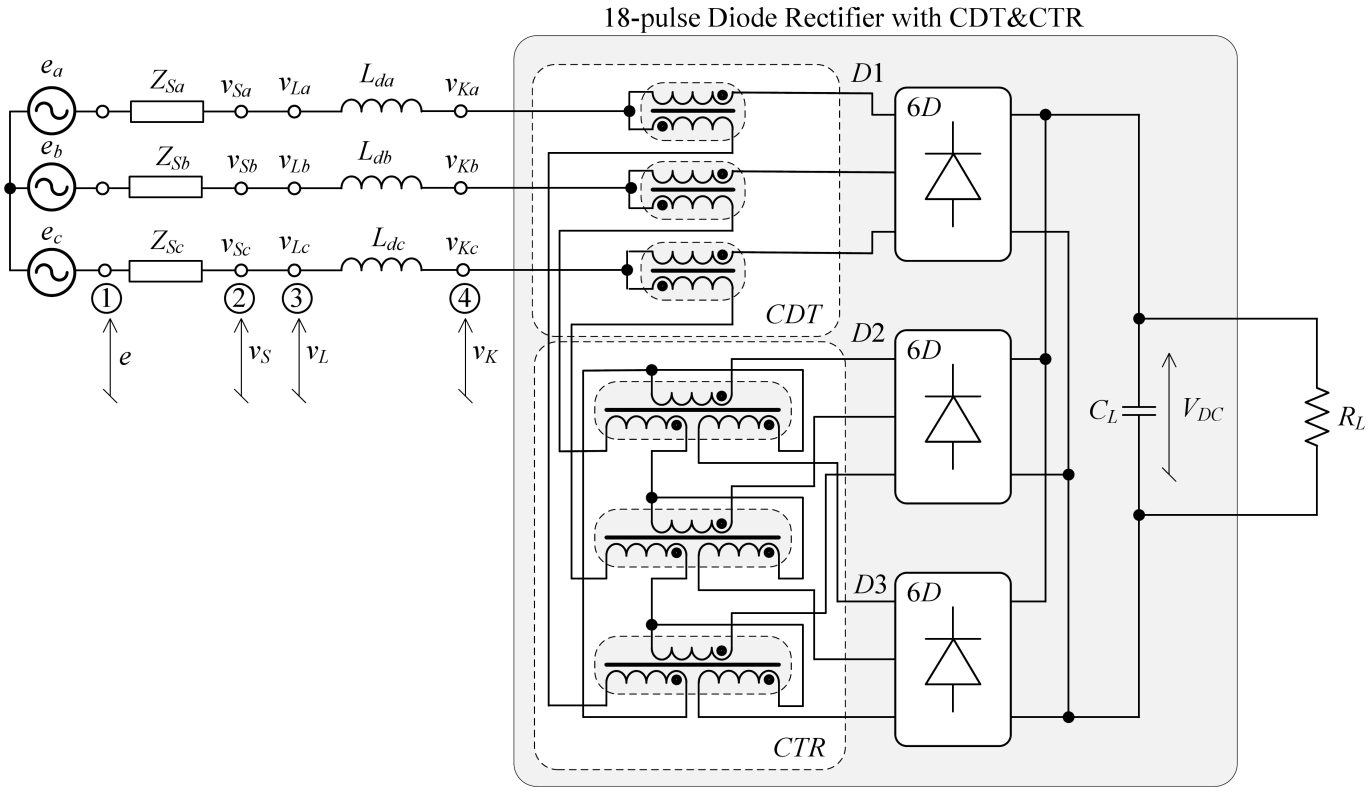

Fig. 1. Supply system on the basis 18-pulse diode rectifier with coupled three-phase reactors (*CDT&CTR*)

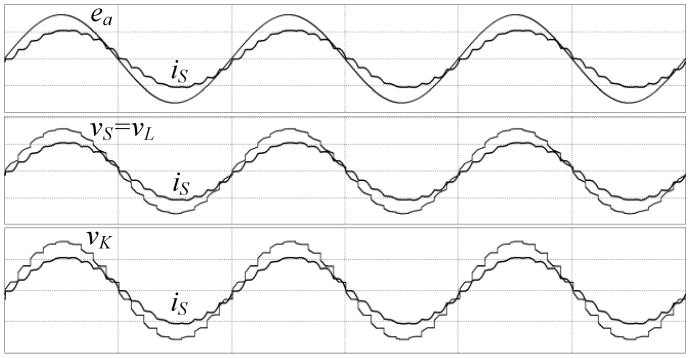

Fig. 2. Typical waveforms of the input voltages and current (200 *V/div*, 40 *A/div*)

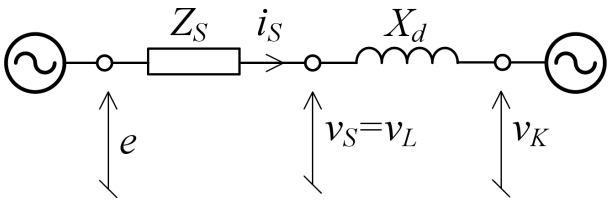

Fig. 3. Simplified model of the system shown in Fig. 1

2.1. Investigation of the mains parameters effect. The coefficient of the input current harmonic distortion is defined by the formula:

$$THD(i_S) = \frac{1}{I_{(1)}}\sqrt{\sum_{h=2}^{\infty} I_{(h)}^2}, \tag{1}$$

where

$$I_{(h)} = \left|\frac{E(jh) - V_K(jh)}{Z_S(jh) + jX_d}\right|, \qquad h = 1,\, 2,\, 3, ... \tag{2}$$

is the h-th harmonic of the input current, and $X_d = \omega L_d$ is the reactance of the network reactor. Hence, assuming the linearity of the network and reactor impedance:

$$Z_S(jh) = R_S + jhX_{S(1)}, \qquad X_d = hX_{d(1)}$$

we get:

$$THD(i_S) = \frac{1}{I_{(1)}}\sqrt{\sum_{h=2}^{\infty} \frac{|E(jh) - V_K(jh)|^2}{R_S^2 + h^2\left(X_{S(1)} + X_{d(1)}\right)^2}}. \tag{3}$$

Since the short-circuit power of the network is:

$$S_{short} = E_{(1)}^2 \Big/ \sqrt{\left(R_S^2 + X_{S(1)}^2\right)},$$

then if $R_S^2 \ll X_S^2$ then $E_{(1)}^2 \Big/ S_{short} \approx X_{S(1)}$. In this case the relation (3) takes the form:

$$THD(i_S) \approx \frac{S_{short}}{I_{(1)}}\sqrt{\sum_{h=2}^{\infty} \frac{|E(jh) - V_K(jh)|^2}{h^2\left(E_{(1)}^2 + S_{short}X_{d(1)}\right)^2}} \tag{4}$$

Equation (4) describes the coefficient $THD(i_S)$ as a function of the inductance L_d of the line reactor and the short-circuit power S_{short} of the supply network. Since:

$$P_{rec} \approx I_{(1)}E_{(1)}$$

then the dependence of $THD(i_S)$ on the power load P_{rec} (for the linear CDT&CTR) is given by the formula:

$$THD(i_S) \approx \frac{S_{short}E_{(1)}}{P_{rec}}\sqrt{\sum_{h=2}^{\infty} \frac{|E(jh) - V_K(jh)|^2}{h^2\left(E_{(1)}^2 + S_{short}X_{d(1)}\right)^2}}. \tag{5}$$

The relations (4) and (5) are confirmed by the functional dependence set on the basis of detailed simulation studies and illustrated in Figs. 4 and 5.

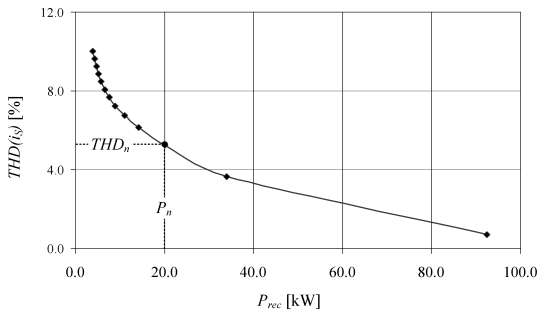

Fig. 4. $THD(i_S)$ versus load power P_{rec} for the linear CDT&CTR (S_{rec}=*400kVA*, L_d=*0.6mH*, sinusoidal input voltage)

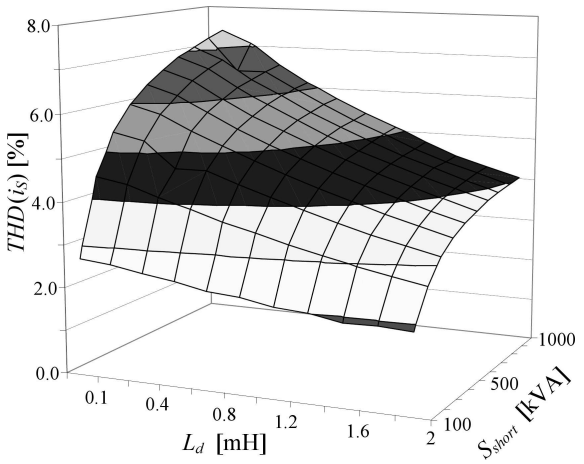

Fig. 5. Variation of the $THD(i_S)$ depending on short-circuit power S_{short} and inductance L_d ($P_{rec} = 20$ kW, sinusoidal input voltage)

It should be noticed that the coefficient $THD(i_S)$ is not most appropriate for assessing the impact of the receiver onto other loads connected to the same supply line. A better criterion, taking into account the effect of the short-circuit power, is the ratio:

$$\frac{THD(i_S)}{S_{short}} \approx \frac{1}{I_{(1)}}\sqrt{\sum_{h=2}^{\infty} \frac{|E(jh) - V_K(jh)|^2}{h^2\left(E_{(1)}^2 + S_{short}X_{d(1)}\right)^2}}. \tag{6}$$

Figure 6 shows above mentioned ratio variations vs. inductance L_d and power S_{short}, determined from the simulations. The trends of this variation are similar to changes of the total voltage harmonic distortion coefficient at the rectifier input, shown in Fig. 7. This leads to the conclusion about the possibility of assessing the impact of the test load onto other loads using the $THD(i_S)/S_{short}$ ratio.

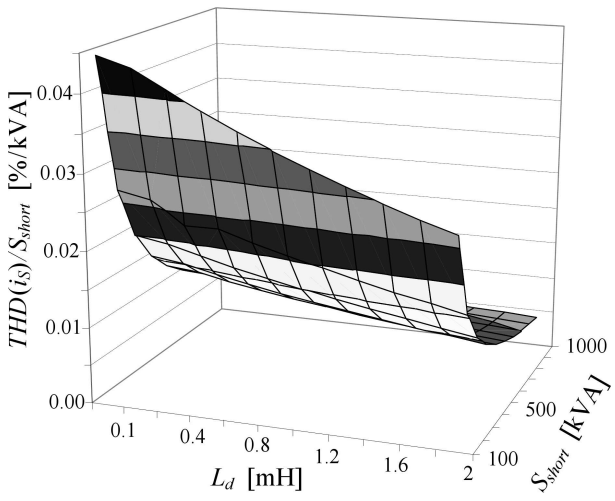

Fig. 6. Dependence of the $THD(i_S)$ to S_{short} ratio versus short-circuit power S_{short} and inductance L_d ($P_{rec} = 20$ kW, sinusoidal input voltage)

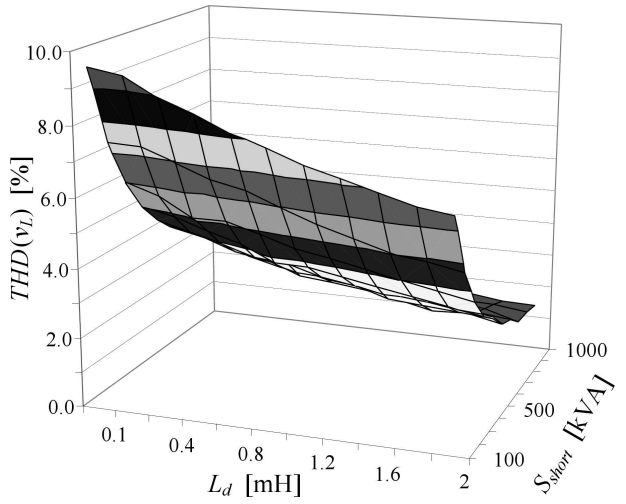

Fig. 7. Variation of the *THD*(v_L) depending on short-circuit power S_{short} and inductance L_d

2.2. Power voltage disturbances effect. The characteristics of the system shown in Fig. 1 also strongly depend on the disturbances of the supply voltage: its harmonic distortion and unbalance. The appearance of those disturbances, even normative, results in a considerable increase of distortion of the input current i_S. This effect can be explained using the model shown in Fig. 3. In particular, it is noticeable that the effect of the distortion of the supply voltage on the deformation of the input current is larger for lower harmonics. It is related with the filtering properties of the reactor L_d and impedance Z_S. This is confirmed by the changes of the coefficient *THD*$''(i_S)$ (in relation to *THD*(i_S) representing the symmetrical sinusoidal voltage supply) as functions of the amplitudes of selected h-order harmonics, shown in Fig. 8. Initial slower increase of the *THD*$''(i_S)$/*THD*(i_S) ratio results from relatively small changes of voltage harmonics v_K at rectifier's terminals (Fig. 3).

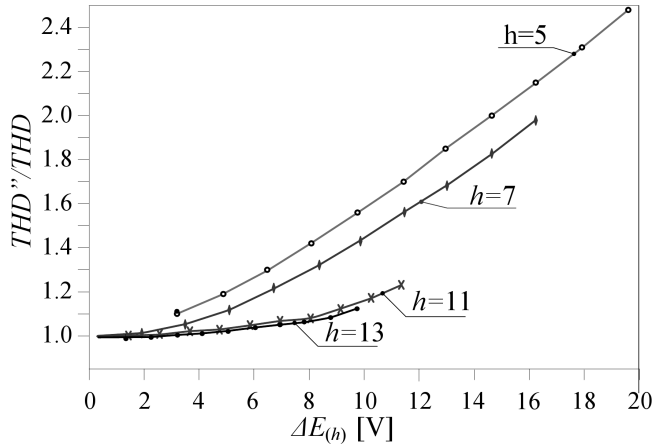

Fig. 8. Relative increase of the *THD*$''(i_S)$ versus amplitude of single harmonics of the power voltage

It is noteworthy that the investigations reported in the present and further chapters refer to one short-circuit power $S_{short} = 400$ kVA and they illustrate only qualitative effects of supply voltage disturbances. That is why the quality of the supply current taken from the network was assessed using the more traditional coefficient *THD*(i_S) instead of *THD*(i_S)/S_{short}.

The change of the voltage v_K is also a direct cause of distortion of the current i_S in case of unbalance of the supply voltage. This unbalance changes the diode conduction intervals in all bridge rectifiers of the investigated system (Fig. 1). As a result, after summing up of the component voltages by the reactors CDT&CTR, the waveforms of the voltages v_K differ from the sinusoid. The dominating harmonic in their spectrum is the third harmonic. This harmonic is also a major cause the distortion of current i_S.

In order to assess more precisely the effect of supply unbalance on the distortion of the current i_S, simulation investigations were carried out in which the unbalance voltage was obtained in the way shown in Fig. 9. The simulation results included changes of the *THD*$''(i_S)$ coefficient (in relation to *THD*(i_S) for the sinusoidal and symmetrical supply voltage) as a function of the amplitude ΔE and phase γ of the booster voltages, shown in Fig. 10. Noticeable is the much larger effect of the amplitude unbalance than that of the phase unbalance.

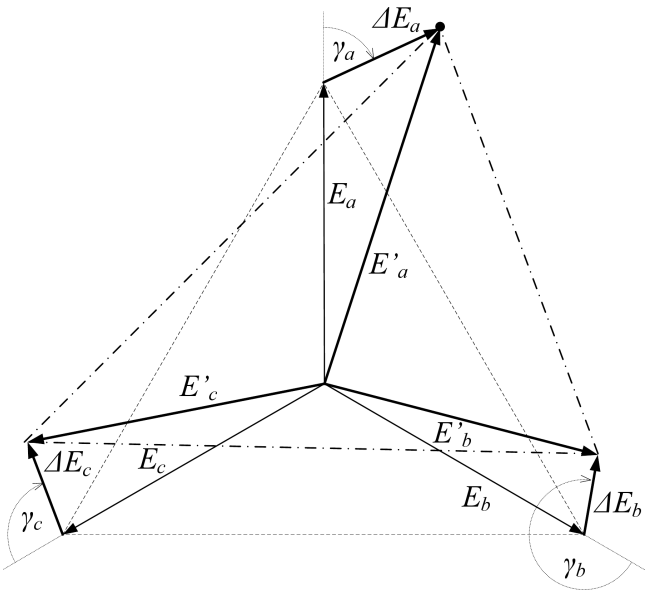

Fig. 9. Phasor variation of the power voltage during tests of the power voltage unbalance effect

Based on the above presented results we can conclude that the multi-pulse rectifiers with coupled reactors, including the investigated 18-pulse system, are good solutions of "clean power converter" type only for the symmetrical and sinusoidal supply voltage [12]. When the supply voltage does not meet these two conditions, even if the disturbances are within normative limits, it results in remarkable distortions of the network current. In those cases it is advisable to use an additional small series active filter [4, 15].

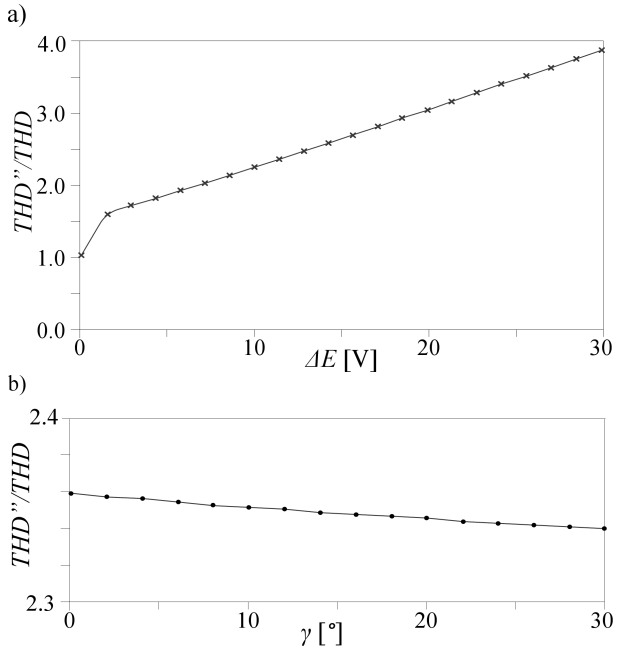

Fig. 10. Relative increase of the *THD*(i_S) in cases of the power voltage unbalance: a) changes of the booster voltages amplitude $\Delta E = \Delta E_a = -\Delta E_c$ for $\gamma_a = \gamma_b = \gamma_c = 0$; b) changes of the booster voltages phase γ for $\Delta E = \Delta E_a = \Delta E_b = \Delta E_c = 30$ V and $\gamma = \gamma_a = \gamma_b = \gamma_c$

3. Integrated robust system

Figure 11 shows the AC/DC supply system constructed using an 18-pulse rectifier with CDT&CTR and integrated with a series active power filter (S-APF) of relatively small power [3, 4, 12, 15]. The applied S-APF system comprises three single-phase bridge inverters (with booster transformers *Tr* and filtering condensers C_F) which were connected to the rectifier output using DC circuits, as was shown in Fig. 12. This system provided opportunities for implementation of the 3-level PWM algorithms, and did not require controlling the active power flow between S-APF and the rectifier, due to the fact that this flow is relatively small and naturally tends to self-stabilising reduction.

3.1. Control method. The S-APF system in the supply system shown in Fig. 11 is controlled by blocking the undesired harmonic components. For those harmonics the system should reveal very large impedance (equal to infinity in theory), while for the required component – the basis harmonic – very small impedance (zero in theory). Therefore the booster voltage v_F in each phase (Fig. 11) should be proportional to the undesired components i_S of the electric current i_S in the same phase. This principle of control is given by the formula:

$$\boldsymbol{v}_F = K \cdot \tilde{\boldsymbol{i}}_S, \tag{7}$$

where K is the proportionality coefficient in [Ω]. In the 3-phase system we take into account that:

$$\boldsymbol{v}_F = \begin{bmatrix} v_{Fa(ref)}(j\omega) \\ v_{Fb(ref)}(j\omega) \\ v_{Fc(ref)}(j\omega) \end{bmatrix}, \qquad \tilde{\boldsymbol{i}}_S = \boldsymbol{G}(j\omega) \cdot \begin{bmatrix} i_{Sa}(j\omega) \\ i_{Sb}(j\omega) \\ i_{Sc}(j\omega) \end{bmatrix}$$

and

$$\boldsymbol{G}(j\omega) = \begin{bmatrix} 1 & 0 \\ \frac{1}{2} & \frac{\sqrt{3}}{2} \\ \frac{1}{2} & -\frac{\sqrt{3}}{2} \end{bmatrix} \cdot \boldsymbol{H}(j\omega) \cdot \begin{bmatrix} 1 & -\frac{1}{2} & -\frac{1}{2} \\ 0 & -\frac{\sqrt{3}}{2} & -\frac{\sqrt{3}}{2} \end{bmatrix}$$

where $\boldsymbol{H}(j\omega)$ is the transmittance of the high-pass filter (HPF) which separates the blocked network current harmonics in the $\alpha-\beta$ coordinate system. This transmittance determines basic blocking abilities of the S-APF system. In 3-phase systems, reasonable options are the $\boldsymbol{H}(j\omega)$ realisations making use of the Clark-Park transformation.

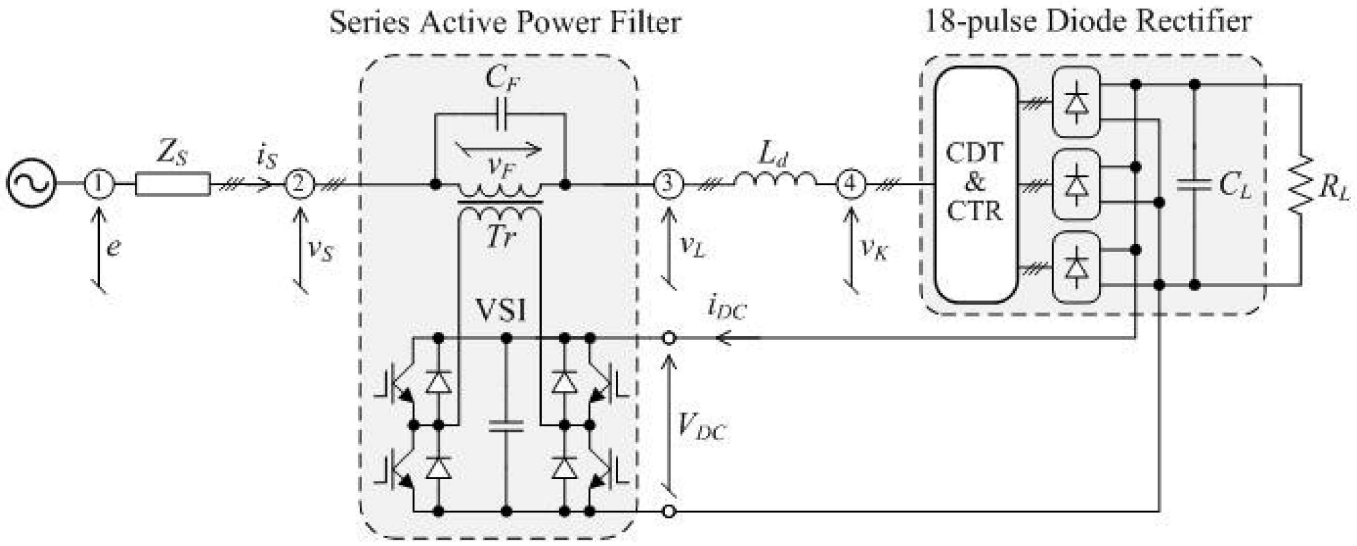

Fig. 11. Supply system integrated with the series active power filter

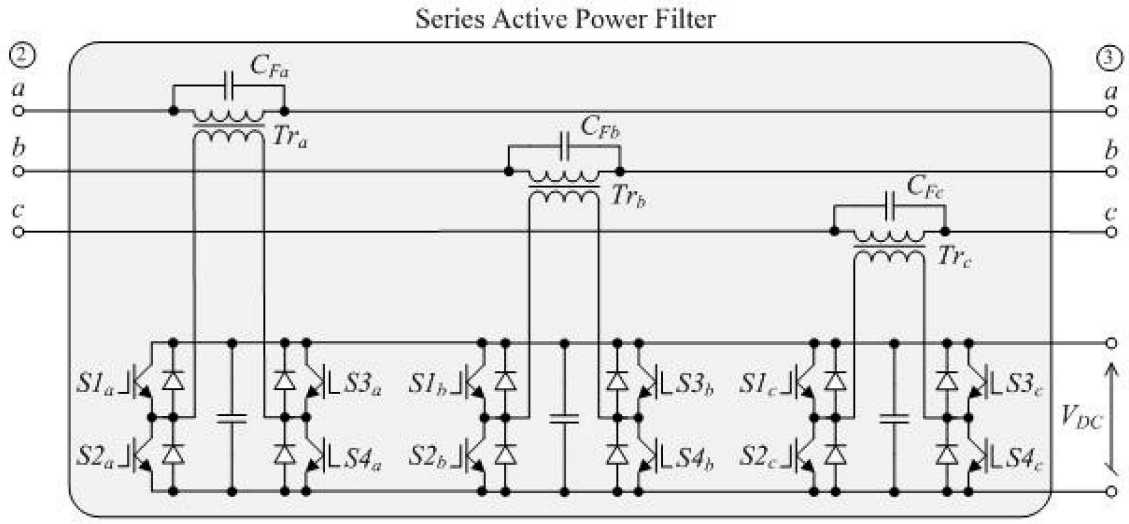

Fig. 12. Application circuits of the series active power filter

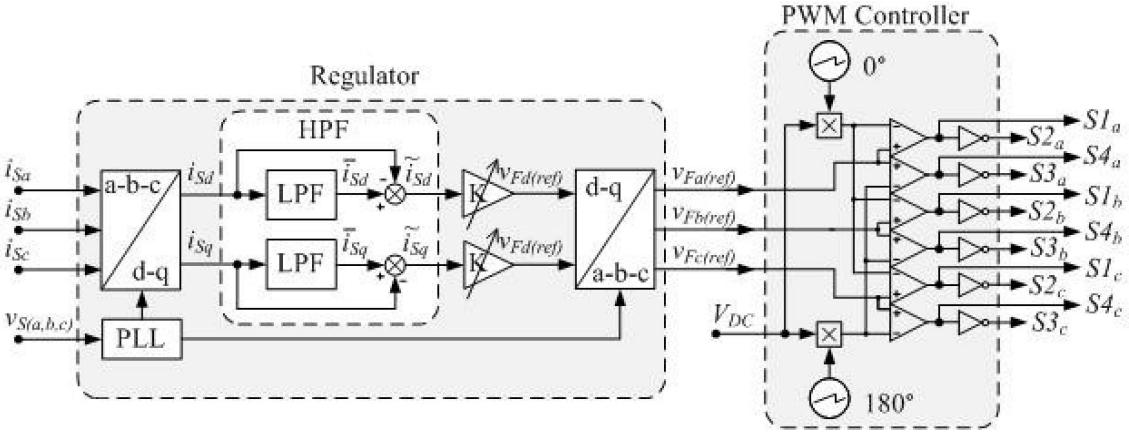

Fig. 13. Basic control system of the series active power filter

In the simplest case shown in Fig. 13, HPF is fully executed in the rotating coordinates $d-q$ based of the difference of the constant components extracted by the 1-st order low-pass filters (LPF) and the non-filtered signals. For this solution, $\boldsymbol{H}(j\omega)$ in the $\alpha-\beta$ coordinate system acc. to [14] has the form:

$$\boldsymbol{H}(j\omega)=\frac{\begin{bmatrix}\omega_C+j\omega & -\omega_S\\ \omega_S & \omega_C+j\omega\end{bmatrix}\cdot\begin{bmatrix}j\omega & \omega_S\\ -\omega_S & j\omega\end{bmatrix}}{\omega_S^2+(\omega_C+j\omega)^2}, \quad (8)$$

where ω_S – network frequency, ω_C – LPF cut-off frequency. Unfortunately, a disadvantage of this solution is the appearance of remarkable through couplings between the filtered harmonic current components $i_{S\alpha}$, $i_{S\beta}$.

A most favourable transmittance $\boldsymbol{H}(j\omega)$ can be obtained by extracting only the constant components using LPF in the $d-q$ coordinate system. Based on those components and making use of the inverse Park transformation we determine the sinusoidal waveforms in the $\alpha-\beta$ coordinates.

The difference between the obtained sinusoidal waveforms and those unfiltered, in the $\alpha-\beta$ coordinates, is the result of the filtration: extraction of higher harmonics. In this case the transmittance $\boldsymbol{H}(j\omega)$ is given acc. to [14] by the formula:

$$\boldsymbol{H}(j\omega)=\mathbf{1}-\frac{\begin{bmatrix}\omega_C+j\omega & -\omega_S\\ \omega_S & \omega_C+j\omega\end{bmatrix}\cdot\omega_C}{\omega_S^2+(\omega_C+j\omega)^2}. \quad (9)$$

A common disadvantage of the transmittances $\boldsymbol{H}(j\omega)$ given by formulas (8) and (9), and connected with possible non-symmetry of the supply voltage of the system shown in Fig. 11, is partial non-filtering of the negative sequence component of the basic harmonic. This results in partial blocking of this component, which excessively increases the overall power of the S-APF system. A reasonable solution here is the realisation of the transmittance $\boldsymbol{H}(j\omega)$ in the way similar to that given by formula (9), but done separately for the positive and negative sequence components. We can write this division as:

$$\boldsymbol{H}(j\omega)=\mathbf{1}-\mathbf{D}_p(j\omega)-\mathbf{D}_n(j\omega), \quad (10)$$

where acc. to [14]:

$$\boldsymbol{D}_p(j\omega) = \frac{\begin{bmatrix} \omega_C + j\omega & -\omega_S \\ \omega_S & \omega_C + j\omega \end{bmatrix} \cdot \omega_C}{\omega_S^2 + (\omega_C + j\omega)^2}, \qquad (11)$$

$$\boldsymbol{D}_n(j\omega) = \frac{\begin{bmatrix} \omega_C + j\omega & \omega_S \\ -\omega_S & \omega_C + j\omega \end{bmatrix} \cdot \omega_C}{\omega_S^2 + (\omega_C + j\omega)^2}. \qquad (12)$$

Hence, after placing (11) and (12) into (10) acc. to [14] we get:

$$\boldsymbol{H}(j\omega) = \frac{\begin{bmatrix} 1 & 0 \\ 0 & 1 \end{bmatrix} \cdot \left((j\omega)^2 + \omega_S^2 - \omega_C^2\right)}{\omega_S^2 + (\omega_C + j\omega)^2}. \qquad (13)$$

It results from formula (13) that the components $i_{S\alpha}$ and $i_{S\beta}$ are filtered in the same way. Consequently, when we use HPF with transmittance (13), the booster voltages v_F in each phase are given by the relation:

$$v_{F(a,b,c)} = K \cdot \frac{\left((j\omega)^2 + \omega_S^2 - \omega_C^2\right)}{\omega_S^2 + (\omega_C + j\omega)^2} \cdot i_{S(a,b,c)}.$$

3.2. Simulation results. Figures 14 and 15 show sample simulation results for the supply system shown in Fig. 11. The simulations were performed using the package PSIM Version 8.0.4. The presented results illustrate the action of the system with the S-APF system switched off and on, for the supply voltage deformation (Fig. 14) and supply voltage non-symmetry (Fig. 15). In both cases the basic S-APF control system was used (Fig. 13). Using the simplest transmittance HPF (8) was dictated by the main goal of the simulation, which was assessing the functionality and features of the proposed solution, without any attempt to optimise dynamic and size parameters – a goal planned for the nearest future.

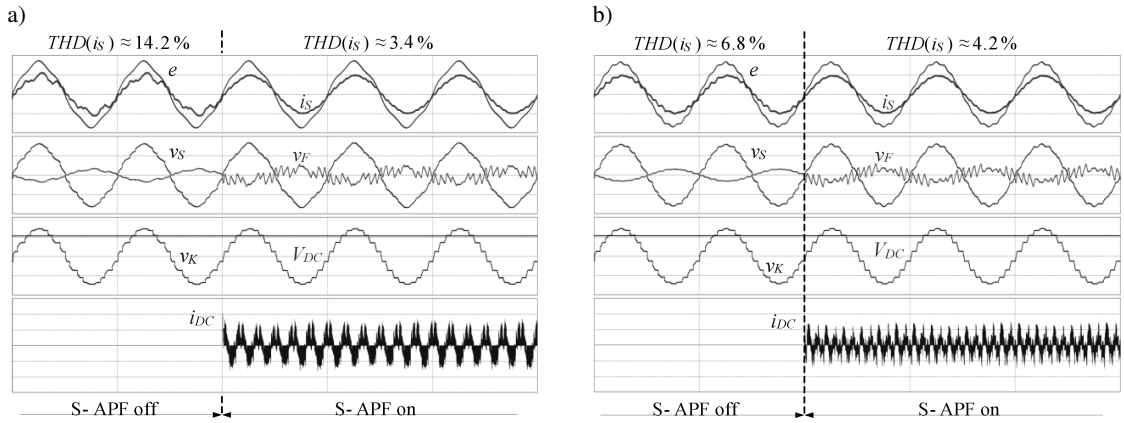

Fig. 14. Voltages and currents in the supply system (Fig.11) with S-APF switched off and on, for supply voltage deformation: a) 5-th harmonic of 6% in magnitude, b) 13-th harmonic of 3% in magnitude (e, v_S, $v_K \rightarrow 200$ *V/div*; $v_F \rightarrow 100$ *V/div*; $V_{DC} \rightarrow 400$ *V/div*; $i_S \rightarrow 50$ *A/div*; $i_{DC} \rightarrow 5$ *A/div*)

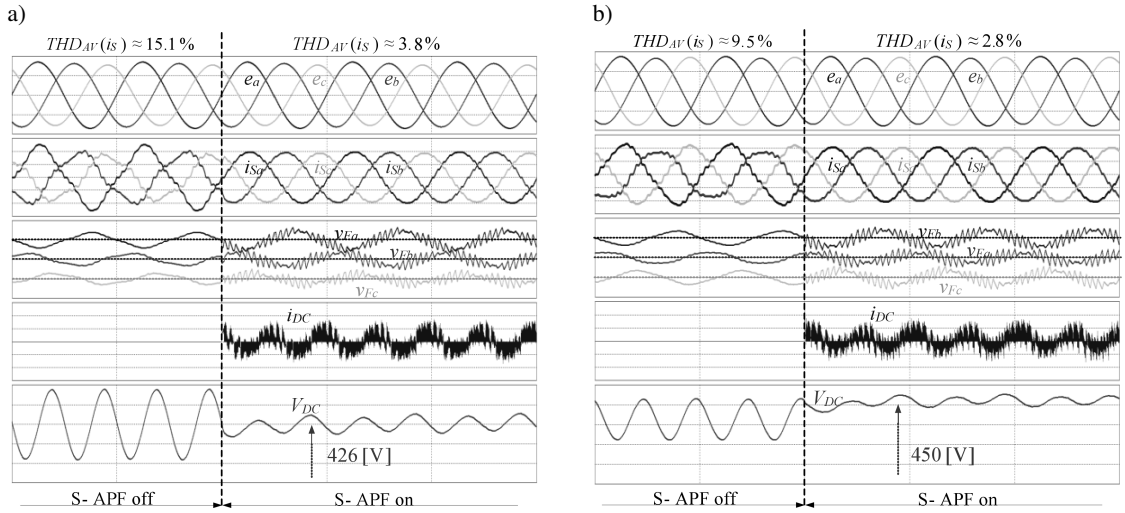

Fig. 15. Voltages and currents in the supply system (Fig. 11) with S-APF switched off and on, for supply voltage non-symmetry: a)$\Delta E_a = \Delta E_b = 30$ [V], $\Delta E_c = 0$ [V], $\gamma_a = \gamma_c = 0^\circ$, $\gamma_b = 180^\circ$; b) $\Delta E_a = \Delta E_b = 30$ [V], $\Delta E_c = 0$ [V], $\gamma_a = \gamma_c = \gamma_b = 0^\circ$ ($e \rightarrow 200$ *V/div*; $i_S \rightarrow 20$ *A/div*; $v_F \rightarrow 100$ *V/div*; $i_{DC} \rightarrow 5$ *A/div*; $V_{DC} \rightarrow 2$ *V/div*)

Table 1 collects the basic parameters of the examined system (Fig. 11), which were recorded in the simulation. These parameters describe the action of the system in the conditions shown in Figs. 14 and 15, and refer to the situation before and after switching S-APF on. Along with the average $THD_{AV}(i_S)$ values, the presented data include the $THD(i_S)$ values calculated for each phase, and the overall powers of the receiver S_{REC} and the series active power filter S_{APF}. It is noteworthy that in each case the overall power S_{APF} is approximately equal to only 10% of the overall power S_{REC}.

Table 1
Basic parameters of the integrated supply system (Fig. 11), before/after switching S-APF On

Parameter	Conditions of system operation, acc. to Figures			
	Fig. 14a	Fig. 14b	Fig. 15a	Fig. 15b
S-APF	off/on	off/on	off/on	off/on
S_{REC} [kVA]	18.3/18.3	18.2/18.2	18.1/18.1	20.5/20.5
S_{APF} [kVA]	0/1.872	0/1.653	0/1.7	0/1.89
S_{APF}/S_{REC}[%]	0/10.2	0/9.1	0/9.3	0/9.2
$THD(i_{Sa})$ [%]	14.1/3.4	6.4/4.6	12.7/3.6	9.1/2.8
$THD(i_{Sb})$ [%]	14.1/3.4	6.4/4.6	16.9/3.8	10.5/2.8
$THD(i_{Sc})$ [%]	14.1/3.4	6.4/4.6	15.6/3.8	8.6/2.7
$THD_{AV}(i_S)$ [%]	14.1/3.4	6.4/4.6	15.1/3.8	9.1/2.8

4. Experimental results

The basic goal of the experimental investigations was practical verification of the efficiency of operation of the proposed system (Fig. 11) in steady-state conditions. The investigations were performed for the case of S-APF integration with the 18-pulse rectifier of power $S_{REC} = 20$ [kVA], and an additional network reactor $L_d = 0.6$ [mH].

Fig. 16. View of the laboratory model of the supply system shown in Fig. 11

Figure 16 shows a laboratory model (made by authors of this article) of the supply system constructionally integrated with S-APF localised at the bottom of the cubicle. In the system the booster transformers *Tr* (Fig. 12) with the transformation ratio 1:12 were used. Therefore, taking into account the voltage $V_{DC} \approx 500$ [V], the amplitude of the booster voltages u_F did not exceed 45 V. The phase current waveforms i_{Sa}, i_{Sb}, i_{Sc} recorded in nominal conditions of this model operation and their spectra before and after switching S-APF on, are shown in Fig. 17. Figures 18 and 19 show the same data, but for 75% and 125% of the nominal load. Their analysis clearly confirms high efficiency of the proposed solution for improving the shape of the network current. It is also noticeable that almost half of the volume of the assembly cubicle (Fig. 16) is occupied by auxiliary connecting elements.

This indicates the potential for more compact constructions of similar systems, revealing good mass and size parameters.

As the supplement to the results shown in Figs. 17–19, Table 2 collects the measured phase shifts angles φ_{Sa}, φ_{Sb}, φ_{Sc}

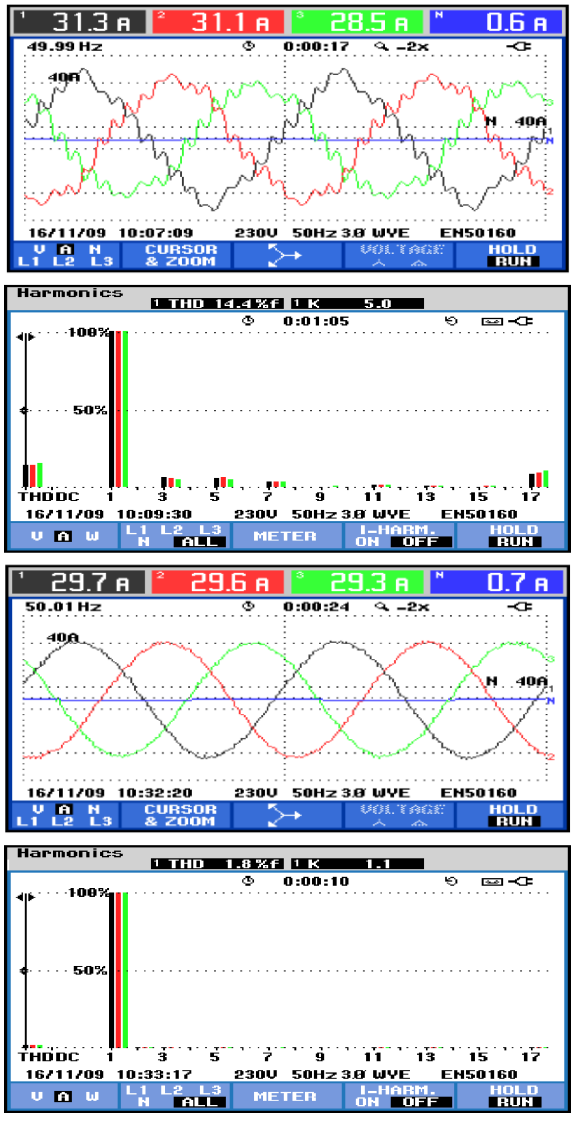

Fig. 17. Oscillograms and spectra of network currents $i_{Sa,b,c}$ in the system of power $S_{REC} = 20$ kVA (nominal load) with reactor $L_d = 0.6$ [mH], before and after switching S-APF on

of the currents i_{Sa}, i_{Sb}, i_{Sc} with respect to the phase voltages v_{Sa}, v_{Sb}, v_{Sc} (additional measurements), and the rms values I_{Sa}, I_{Sb}, I_{Sc} of these currents, for three different loads: 100%, 125% and 75% of the nominal load, and for S-APF switched off and on. The presented data also include average values $\cos\varphi_{AV} = (\cos\varphi_a + \cos\varphi_b + \cos\varphi_c)/3$. These results indicate an additional effect of the action of the S-APF system, which is levelling of the rms values and phase shift angles of the network currents. Moreover, the recorded $\cos\varphi_{AV}$ values confirm the energy related advantages of the examined solution.

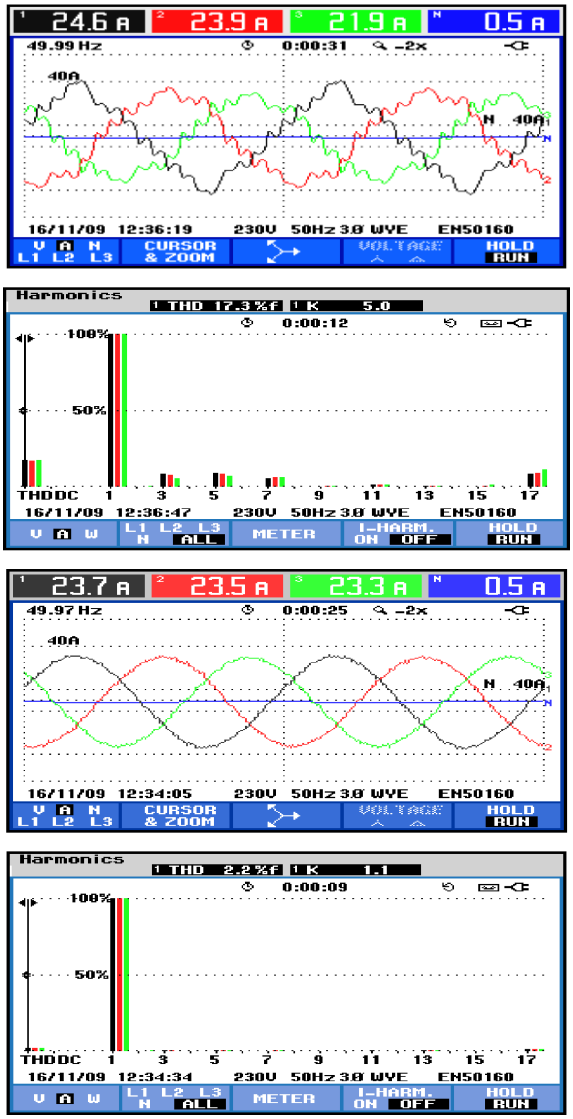

Fig. 18. Oscillograms and spectra of network currents $i_{Sa,b,c}$ in the system of power $S_{REC} = 15$ kVA (75% of nominal load) with reactor $L_d = 0.6$ [mH], before and after switching S-APF on

By confirming the results of the simulation calculations, the presented results of the laboratory measurements make it possible to conclude that also in real conditions the series active power filter can remarkably reduce higher harmonics of the network current of the 18-pulse converter with CDT&CTR.

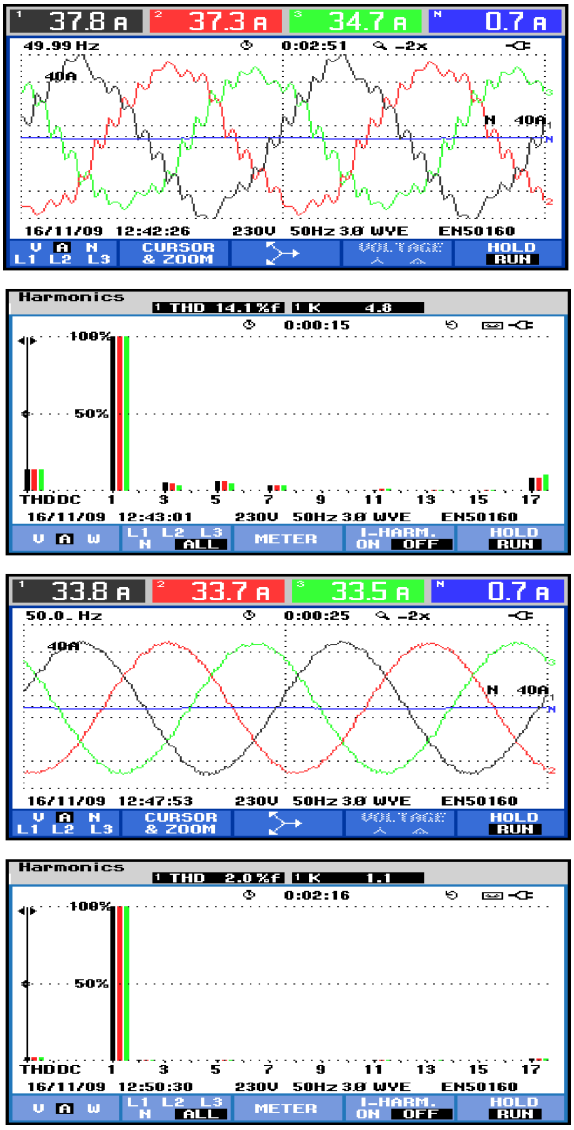

Fig. 19. Oscillograms and spectra of network currents $i_{Sa,b,c}$ in the system of power $S_{REC} = 25$ kVA (125% of nominal load) with reactor $L_d = 0.6$ [mH], before and after switching S-APF on

Table 2
Phase shift angles and RMS nalues of the supply currents i_s, and the $\cos\varphi_{AV}$ in the experimental setup, for 75%, 100% and 125% of the nominal load

S-APF	$\frac{\varphi_a\ [^\circ]}{I_{Sa}\ [A]}$	$\frac{\varphi_b\ [^\circ]}{I_{Sa}\ [A]}$	$\frac{\varphi_b\ [^\circ]}{I_{Sb}\ [A]}$	$\cos\varphi_{AV}$
Load 75%				
On	20/23.7	18/23.5	19/23.3	0.946
Off	18/24.6	11/23.9	16/21.9	0.966
Load 100%				
On	16/29.3	16/29.5	17/29.7	0.959
Off	11/28.2	8/31	13/31.1	0.983
Load 125%				
On	15/33.8	14/33.7	15/33.5	0.967
Off	11/37.8	5/37.3	8/34.7	0.991

S-APF is efficient in cases of nominal load and in under- or overload states. Moreover, the integration of the rectifier

with S-APF in the examined supply system makes it possible to simplify the structure of the converter, by resignation from the network reactor L_d, and simultaneous remarkable reduction of the negative effect on the supply network.

5. Conclusions

The application of the 18-pulse converter with the system of coupled reactors cooperating with a low-power series active power filter seems to be an interesting solution for the problem of clean AC-DC energy conversion, due to:

- simplification of the converter system resulting from possible elimination of the network reactor,
- small overall power of the both systems [4], decreasing their costs,
- remarkable reduction of the content of higher harmonics in the supply current waveform,
- small susceptibility of the system to supply asymmetry and load changes,
- potential for construction of low-cost and high-reliability supply systems.

The advantages resulting from the application of the presented filter system refer to efficient minimisation of the negative action of the multi-pulse converter onto the supply network, in various supply conditions. We can assume that the 18-pulse rectifier in the configuration with a series active power filter compose a converter system working in conditions close to CPC.

REFERENCES

[1] A. Moreno-Muńoz, *Power Quality Mitigation Technologies in a Distributed Environment*, Springer-Verlag, London, 2007.

[2] R. Strzelecki and G. Benysek, *Power Electronics in Smart Electrical Energy Networks*, Springer-Verlag, London, 2009

[3] R. Strzelecki and H. Supronowicz, *Power Factor in AC Supply Systems and Improvements Methods*, Publishing House of the Warsaw University of Technology, Warsaw, 2000, (in Polish).

[4] H. Akagi, E.H. Watanabe, and M. Aredes, *Instantaneous Power Theory and Applications to Power Conditioning*, John Wiley&Sons, London, 2007.

[5] D.A. Paice, *Power Electronics Converter Harmonics, Multipulse Methods for Clean Power*, Wiley-IEEE Press, London, 1999.

[6] D.A. Paice, *Clean Power Electronic Converters: Engineering Design and Application Guides*, Paice & Associates, Palm Harbor, 2004.

[7] J.W. Kolar and H. Ertl, "Status of the techniques of three-phase rectifier systems with low effects on the mains", 21^{st} *Int. Telecommunications Energy Conf. INTELEC'99* 1, 16 (1999).

[8] B. Singh, B.N. Singh, A. Chandra, K. Al-Haddad, A. Pandey, and D.P. Kothari, "A review of three-phase improved power quality AC-DC converters", *IEEE Trans. on Indust. Electronics* 51 (3), 641–660 (2004).

[9] B. Singh, S. Gairola, B.N. Singh, A. Chandra, and K.B. Al-Haddad, "Multipulse AC–DC converters for improving power quality: a review", *IEEE Trans. on Power Electronics* 23 (1), 260–281 (2008).

[10] G. Gong, M.L. Heldwein, U. Drofenik, J. Minibock, M. Kazuaki, and J.W. Kolar, "Comparative evaluation of three-phase high power factor AC-DC converter concepts for application in future more electric aircraft", 19^{th} *Annual IEEE Applied Power Electronics Conf. and Exposition APEC* 2, 1152–1159 (2004).

[11] J. Plewako, "Multi-pulse diode converters supplied from autotransformers", *Electrotechnical Review* 2, 53–56 (2007), (in Polish).

[12] P. Mysiak, *Multi-Pulse Diode Rectifier with Current Harmonic Blocking Reactors*, Publishing House of Gdynia Maritime University, Gdynia, 2010.

[13] H. Fujita and H. Akagi, "An approach to harmonic current-free ac/dc power conversion for large industrial loads: the integration of a series active filter with a double-series diode rectifier", *IEEE Trans. Indust. Appl.* 33 (5), 1233–1240 (1997).

[14] F.Z. Peng, H. Akagi, and A. Nabae, "Compensation characteristics of the combined system of shunt passive and series active filters", *IEEE Trans. on Indust. Appl*. 29 (1), 144–151 (1993).

[15] R. Strzelecki and H. Supronowicz, *Filtration of the Harmonic in AC Supply Systems*, Adam Marszałek Publishing House, Toruń, 1997/1999, (in Polish).